A MODEL FOR LOW-p_T PROCESSES BASED ON CLASSICAL STRING DYNAMICS*

BY X. ARTRU

Laboratoire de Physique Théorique et Hautes Energies**, Bât. 211, Université de Paris-Sud, 91405 Orsay, France

(Received October 7, 1985)

We review a recursive fragmentation model of low-p_T jets, based on classical string dynamics, which possesses all the qualitative features of the multiperipheral model and Regge asymptotic behaviour. The parameters of the model are uniquely determined by the Regge trajectories and the reggeon vertex functions. We apply this model to multiparticle states corresponding to the cut reggeons and the cut pomerons.

PACS numbers: 12.40.-y

1. Introduction

Due to the increasing complexity of the final states and of the detector systems in high-energy collisions, the comparison between theory and experiment is more and more often done through Monte-Carlo simulations. In the present paper, I will talk about the simulation of a jet, more precisely a soft jet, which occurs typically in a soft (low-p_T) hadron-hadron collision. I will show that classical string dynamics leads to a recursive fragmentation model which: (*i*) contains all the qualitative features of the multiperipheral model, (*ii*) possesses Regge asymptotic behaviour. The latter property will enable me to fix the recursive fragmentation function, assuming the knowledge of the Regge trajectories and the reggeon vertex functions. I will apply this model to the multiparticle states corresponding to the cut reggeon and cut pomeron, in the context of two-component duality. Finally, I will discuss the theoretical limitations of this model.

I will organize my review as follows: in Section 2, I recall the main qualitative properties of the multiperipheral model and define the most general recursive fragmentation model. In Section 3, I introduce the string picture and show a close connection with the multi-

* Presented at the XXV Cracow School of Theoretical Physics, Zakopane, Poland, June 2–14, 1985.

** Laboratoire associé au Centre National de la Recherche Scientifique.

peripheral model and with the dual resonance model. I establish the Regge asymptotic behaviour in Section 4. In Section 5, I apply the model to the cut reggeon and the cut pomeron and discuss its theoretical limitations. I summarize the results and draw the conclusions in Section 6.

2. *The multiperipheral picture*

The multiperipheral model of Amati, Fubini, Stanghellini and Tonin [1], based on the diagram of Fig. 1, accounts for the main features of high-energy, soft inelastic collisions, namely

(*i*) transverse momentum cut-off, $p_T \lesssim 300$ MeV/c,
(*ii*) leading particle effect,
(*iii*) limiting fragmentation,
(*iv*) rapidity plateau,
(*v*) short range order,
(*vi*) local compensation of charges and of transverse momentum.

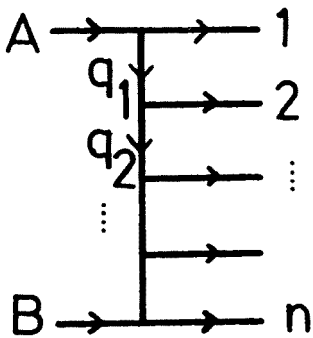

Fig. 1. Multiperipheral diagram for the production of n particles in hadron-hadron collision

According to limiting fragmentation (or Feynman scaling), the leading particle[1] spectrum is of the form

$$f(\vec{p}_{1T}^{\,2}, z_1)d^2\vec{p}_{1T}dz_1/z_1, \tag{2.1}$$

where $z_1 = p_1^+/p_A^+$, $p^\pm = p^0 \pm p^z$, $p_T = (p^x, p^y)$, the z-axis being defined by the beam direction. The recursive fragmentation model [2] iterates the limiting fragmentation down the multiperipheral chain:

$$A \to p_1 + q_1$$
$$\qquad\quad \to p_2 + q_2$$
$$\qquad\qquad\quad \to \ldots$$

[1] "particles" 1, 2 n... in Fig. 1 are not necessarily final particles but can be strongly decaying resonances.

However, unlike p_A, q_i is not on-mass-shell and $q_{iT} \neq 0$; from rotational invariance in the transverse plane and Lorentz boost invariance along the z axis, the most general momentum sharing distribution is of the form[2,3]

$$dP_{q \to p+q'} = f(q^2, \vec{q}_T^2, \vec{p}_T^2, \vec{q}_T'^2, z) d^2 p_T dz/z, \tag{2.2}$$

where $z = p^+/q^+$. Simplified forms for f appear in the literature, for instance, the quark cascade model of Field and Feynman [3] uses $f(\vec{q}_T'^2, z)$.

Forward-backward symmetry. As stressed by Andersson, Gustafson and Söderberg [4], it is important that a recursive model gives the same multiparticle distribution when iterated from top to bottom or from bottom to top in Fig. 1. For the general form (2.2), this requires

$$f = D^{-1}(q^2, \vec{q}_T^2) G(q^2, \vec{q}_T^2, \vec{p}_T^2, \vec{q}_T'^2, q'^2), \tag{2.3}$$

where G is symmetrical in q and q' and D^{-1} is a normalization factor. This does not drastically reduce the choice of f but, as we will see later, it will be very restrictive in the case where f does not depend on q^2.

3. The classical string picture

1. Geometry and kinematics

Now I take an apparently different point of view. I adopt the dual string model [5] and assume that a classical treatment is not too far from reality. The most simple classical mechanism for $A+B \to 1+\ldots+n$ is represented by the duality diagram of Fig. 2a: the incoming strings A and B coalesce at point F, where the quark pair $\bar{q}_A q_B$ annihilate; it results in a single massive string, which I call a "dart"; the dart eventually breaks into several pieces at points $Q_1, Q_2 \ldots Q_{n-1}$, where quark pairs are created. Neglecting quark masses and applying classical rules [6, 7] for string fusion and breaking, one finds [6, 8] that the motion of the dart and of the final strings is essentially one-dimensional, as shown in Fig. 3. Accordingly, the longitudinal motion is well approximated by the $1+1$ dimensional limit of the string model. In this limit, the free string follows the "yoyo" motion shown in Fig. 4 and the whole space-time history of the collision takes the form of Fig. 5. The zigzaging quarks at the end points fill the places of the transverse pieces of string of Fig. 3. Up to subsection 4, I will consider a $1+1$ dimensional world.

There is a simple connection between momentum and configuration spaces. In Fig. 4, the two-vector I I' is equal to p/κ, where κ is the string tension $\simeq 1$ GeV/Fermi, related to the Regge slope by

$$2\pi\kappa\alpha'\hbar = 1. \tag{3.1}$$

---

[2] As one approaches the end of the chain, Feynman scaling is less and less accurate and correction factors dependent on the subenergy $\hat{s} = (q+p_B)^2$ have to be introduced. This will not be treated in the present review.

[3] In this paper, we do not take into account the spin degree of freedom. The flavour one will be introduced at the end of Section 4.

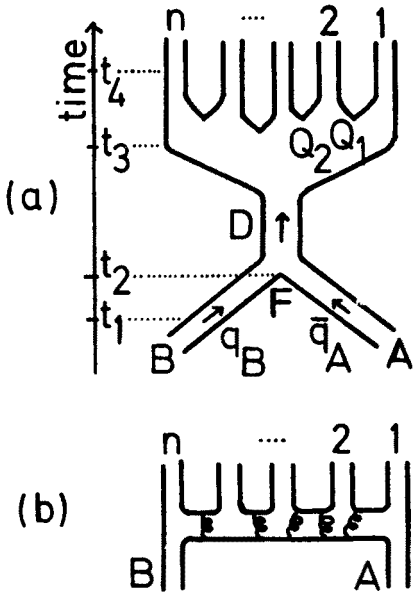

Fig. 2

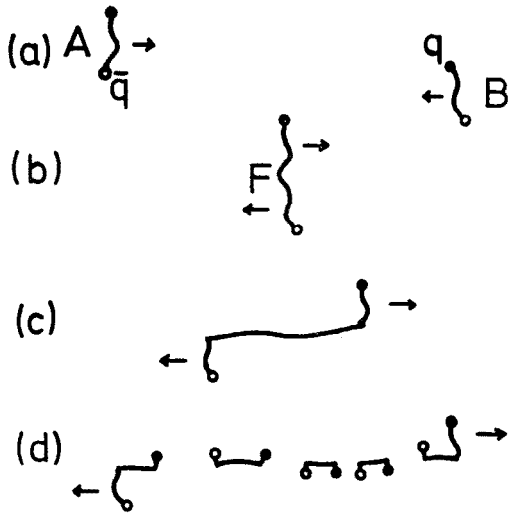

Fig. 3

Fig. 2. Equivalent duality diagrams describing the same reactions as Fig. 1. (a) *s*-channel picture: the incoming strings A and B join at point F to form a "dart" D. At F, the antiquark $\bar{q}_A$ of A annihilates with the quark q_B of B. The dart subsequently breaks at points $Q_1, Q_2, \ldots, Q_{n-1}$, where new quark pairs are created; (b) multiperipheral picture. I have drawn some gluon lines, which are responsible for the binding of the quarks and antiquarks in the exchanged mesons. These diagrams contribute to the "resonant" or "cut-reggeon" cross-section

Fig. 3. Classical mechanism corresponding to the *s*-channel diagram (a) of Fig. 2 (a), (b), (c) and (d) display the shapes of the strings at the times t_1, t_2, t_3 and t_4 indicated in Fig. 2a. These shapes are typically those obtained by solving the classical equations of motion [6–8]

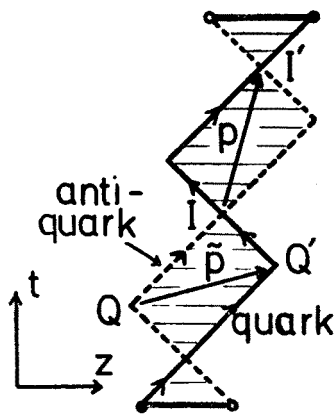

Fig. 4. Motion of a string in 1+1 dimension (yo-yo). The units are such that the string tension κ is equal to one. $\tilde{p}$ = dual of p, i.e. $\tilde{p}^0 = p^z$, $\tilde{p}^z = p^0$

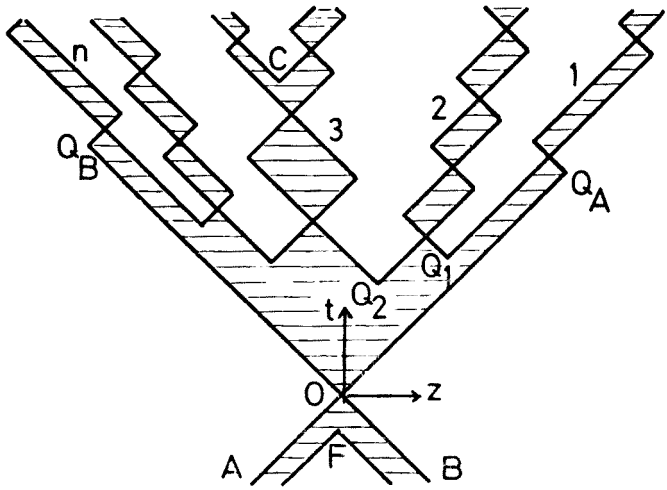

Fig. 5. Classical space-time history corresponding to the s-channel diagram (a) of Fig. 2, in 1+1 dimension

In the following, I shall take units such that $\kappa = 1$. Furthermore QQ' is equal to $\tilde{p}$, the vector dual to p obtained by interchanging p^0 and p^z. More generally, the polygon $OQ_AQ_1 \ldots Q_{n-1}Q_B$ in Fig. 5 is the dual of the closed chain $p_A, -p_1 \ldots -p_n, p_B$ (neglecting p_A^- and p_B^+), and the vectors $OQ_1, \ldots OQ_{n-1}$ are dual to the momentum transfers $q_1, \ldots q_{n-1}$ of the multiperipheral picture (Fig. 1).

2. The breaking prescriptions

Up to now, I have said nothing about the locations of the breaking points $Q_1 \ldots Q_{n-1}$. Let me present two prescriptions, a naive one and the "Lund symmetric" prescription.

a) The naive breaking prescription [6, 8]: *A string can break anywhere at anytime with a probability*

$$dP = \mathscr{P}\, dl\, dt \tag{3.2}$$

per element of length dl and time dt. The parameter $\mathscr{P}$, of the order of a Fermi^{-2}, will be called the "fragility" of the string. We shall often use the parameter

$$b = \mathscr{P}/(2\kappa^2)\ (= \mathscr{P}/2, \text{ in our units}). \tag{3.3}$$

This law is similar to the law for the creation of e^+e^- pairs in a 1+1 dimensional electric field [9] (Schwinger model).

Eq. (3.2) is manifestly Lorentz invariant and forward-backward symmetric. The part of Fig. 5 within, say, a vertical band of 10 Fermi wide about the time axis, looks similar in events with very different values of p_A^+ amd p_B^- provided p_A^+ and $p_B^- > 10$ GeV. This is sufficient for speaking of a rapidity plateau.

Let us now consider in Fig. 5 the chain of breaking points $Q_1, \ldots Q_{n-1}$ which occur in the dart history (thus excluding points like C, which we interpret as resonance decay). It is clear that a breaking point Q preempts new dart decay in its future light cone. One

can then show easily that the density of such points is

$$dN = 2bd^2Q \exp\left[-2b\mathscr{A}(Q)\right], \tag{3.4}$$

where $\mathscr{A}(Q)$ is the area spanned by the dart in the past light cone of Q; the exponential factor is the probability that no preempting breaking point lies in this area. Thus breaking points lie not far from the hyperbola $\mathscr{A}(Q) = 1/2b$ and we have effectively an "inside out" cascade, as was also argued for by Bjorken [10].

Since the vector OQ_i in Fig. 5 is dual to the momentum transfer q_i of the multiperipheral picture (Fig. 1), we have

$$\mathscr{A}(Q_i) = \tfrac{1}{2}\tilde{q}_i^2 = -\tfrac{1}{2}q_i^2 = -\tfrac{1}{2}q_i^+q_i^-. \tag{3.5}$$

Thus, large negative q^+q^- are suppressed by a factor

$$\exp\left(-b|q^+q^-|\right). \tag{3.6}$$

Large $|q^+q^-|$ are also suppressed in the multiperipheral model, owing to the suppression of large

$$-q^2 = -q^+q^- + \vec{q}_\mathrm{T}^2. \tag{3.7}$$

In fact, the main qualitative features of the multiperipheral model, (*i*) to (*vi*) of Section 2, are contained in the naïve string model. Hence, diagram (a) of Fig. 2, which represents the classical string picture of Fig. 5, is "dual" to diagram (b) of Fig. 2, which represents the multiperipheral picture.

Similarly, we can show that the n-particle exclusive distribution is

$$\sigma_{\mathrm{tot}}^{-1}d\sigma = (2b)^{n-1}d^2p_1 \ldots d^2p_n\delta^{(2)}(p_A+p_B-p_1 \ldots -p_n)e^{-2b\mathscr{A}}, \tag{3.8}$$

where $\mathscr{A}$ is the spanned area in the union of the past light cones of $Q_1, \ldots, Q_{n-1}$ in Fig. 5. (3.8) has an important factorization property: *The possible substates emitted between two fixed breaking points Q and Q' (Fig. 6a) have the same relative weights as those emitted by a dart where Q and Q' are the turning points (Fig. 6b).*

The deep reason is causality + the homogeneity of the string : in Fig. 6a, and Fig. 6b, the spacelike dotted curve represents an unbroken piece of string in some curved reference frame; this piece is the relevant initial state for the subsystem QQ'; it is in the same state in Fig. 6a and Fig. 6b.

The model can also be formulated as a recursive one [8, 11], by looking at dart decay in the infinite momentum frame, i.e., taking $X^- = X^0 - X^3$ as time coordinate. The splitting distribution is then

$$dP_{q\to p+q'} = b\exp\left(-bm^2/z\right)dm^2dz/z. \tag{3.9}$$

$m^2/2z$ is the area spanned by the dart since the preceding breaking point in the infinite momentum frame, whence the exponential factor in (3.9). This factor is similar to (3.6) since

$$|q'^+q'^-| \underset{z\to 0}{\sim} m^2/z. \tag{3.10}$$

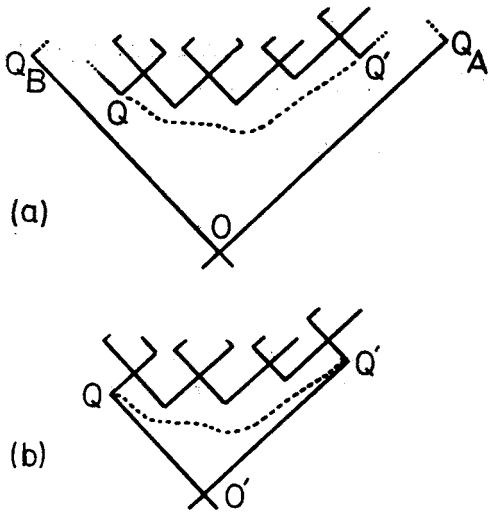

Fig. 6. Illustration of the factorization property which follows from (3.8): the final substate emitted between Q and Q' in diagram (a) and the identical state produced in diagram (b) have the same probability, for fixed Q and Q'

It is clear from (3.9) that the masses of the final strings are not fixed, but have a continuous spectrum extending from zero to infinity, with an exponential cut-off at $m^2 \sim b^{-1}$. This is due to the too great simplicity of the law (3.2) which allows the dart to break at two arbitrarily nearby points. The model may describe the limit $\hbar \to 0$, $g^2 \to 0$ of the dual resonance model when the resonances, whose masses are given by

$$m^2 = (n-\alpha_0)/\alpha' = 2\pi\hbar\kappa(n-\alpha_0)\,(n \text{ integer}), \tag{3.11}$$

become infinitely dense and, for finite n, infinitely narrow.

b) The "symmetric Lund" prescription [4]: If we want the final strings to have the masses of physical particles or resonances, instead of the continuous spectrum implied by (3.9), we must modify the probability law (3.2). Miraculously enough, it is still possible to fulfill limiting fragmentation as well as the factorization property illustrated in Fig. 6. This means that the model is of the recursive type, if, for example, we look at the dart in the infinite momentum frame; the splitting function must be a function only of z, since the dependence on q^2 allowed by (2.2) would spoil our factorization property.

Furthermore we require forward-backward symmetry. This restriction then determines the form of the splitting distribution [4, 12]:

$$f(z)dz/z = N(1-z)^a \exp(-bm^2/z)dz/z. \tag{3.12}$$

Here b is an arbitrary parameter, unlike the constant b appearing in (3.9) which was defined by (3.2)–(3.3), and m is the common mass of all the produced particles. a is a parameter greater than -1 and N a normalization factor.

We note the same $\exp(-2b \times \text{area}) \sim \exp(-b|q'^{+}q'^{-}|)$ damping factor as in (3.9). In fact, one can generalize Eq. (3.12) to allow an arbitrary spectrum of produced particles, which includes (3.12) and (3.9) as special cases [13].

3. Connection between the two prescriptions and the dual resonance model [13]

In the naïve prescription (3.2), the lifetime of a string of mass m can be shown to be

$$\tau = (m\kappa b)^{-1}. \tag{3.13}$$

In the dual model, the resonance has zero width and hence infinite lifetime, in the tree approximation. However, if we take the Regge slope α' to be complex, they acquire a width

$$\Gamma = m \operatorname{Im} \alpha' / \operatorname{Re} \alpha'. \tag{3.14}$$

Since the string tension and the Regge slope are related by

$$\operatorname{Re} \alpha' = (2\pi\hbar\kappa)^{-1}, \tag{3.15}$$

the two results (3.13) and (3.14) agree with, i.e. $\Gamma\tau = \hbar$, provided

$$b = 2\pi \operatorname{Im} \alpha'. \tag{3.16}$$

The connection (3.16) can also be obtained from the fact that the dual model cross sections are damped at large $|q^{+}q^{-}|$ by a factor[4]

$$\exp(-2\pi \operatorname{Im} \alpha' |q^{+}q^{-}|), \tag{3.17}$$

which reduces to (3.6) with the identification (3.16).

4. Generalization to flavour and transverse degrees of freedom

(3.12) can be generalized to $1+3$ dimensions and several flavours [4, 13] by choosing a splitting function of the form

$$f_{kl}^{h}(\vec{q}_T^{\,2}, \vec{p}_T^{\,2}, \vec{q}_T'^{\,2}, z) = d_k^{-1}(\vec{q}_T^{\,2})\,(z/\mu^2)^{a_k(\vec{q}_T^{\,2})}$$

$$\times g_{kl}^{h}(\vec{q}_T^{\,2}, \vec{p}_T^{\,2}, \vec{q}_T'^{\,2})\,(1/z-1)^{a_l(\vec{q}_T'^{\,2})} \exp(-b\mu^2/z), \tag{3.18}$$

where h, k and l label the internal quantum numbers carried by p, q and q', g is symmetrical in the interchange $q, k \leftrightarrows q', l$, $\mu = \sqrt{m_h^2 + \vec{p}_T^{\,2}}$ is the transverse energy of the hadron and the factor d^{-1} normalizes the total splitting probability to unity. Note that f is again independent of q^2. "Transverse softness" requires g to be a strongly decreasing function of $\vec{q}_T^{\,2}$ and $\vec{q}_T'^{\,2}$.

[4] Eq. (3.17) has been checked [13] for the elastic cross section and the leading particle spectrum.

4. Asymptotic Regge behaviour

Let one rapidity gap ΔY_i in the multiperipheral chain be large; then

$$(p_i+p_{i+1})^2 \sim |q_i^+ q_i^-|^{-1} \sim (1-z_i)^{-1} \sim e^{\Delta Y_i}. \tag{4.1}$$

From (3.18) and (4.1), we see that the probability that ΔY_i be larger than some Δ is

$$P(\Delta Y_i > \Delta) \propto \exp\{-[1+a_i(\vec{q}_{iT}^2)]\Delta\}. \tag{4.2}$$

This result (4.2) coincides with the prediction of Regge theory, which applies for large ΔY_i [14], if we make the identification [13]

$$a_i(\vec{q}_T^2) = \alpha_{out} - 2\alpha_i(t = -\vec{q}_T^2), \tag{4.3}$$

where $\alpha_i(t)$ is the exchanged trajectory and α_{out} the intercept of the "output trajectory" defined by

$$\sigma_{tot} \propto s^{\alpha_{out}-1}. \tag{4.4}$$

More generally, we can show that our model possesses multi-Regge and triple-Regge behaviours, where the reggeon-particle-reggeon vertex $\gamma_{kl}^h(t, \mu^2, t')$ and the triple-Regge vertex $\gamma_{k,k,out}(t)$ and related to the functions g_{kl}^h and d_k of (3.18) by [15]

$$\frac{g_{kl}^h(\vec{q}_T^2, \vec{p}_T^2, \vec{q}_T'^2)}{\sqrt{d_k(\vec{q}_T^2)d_l(\vec{q}_T'^2)}} = \mu^{2\alpha_{out}} e^{b\mu^2} |\gamma_{kl}^h(-\vec{q}_T^2, \mu^2, -\vec{q}_T'^2)|^2, \tag{4.5}$$

$$d_k(\vec{q}_T^2) = \gamma_{k,k,out}^2(-\vec{q}_T^2). \tag{4.6}$$

Thus our model possesses all the Regge asymptotic limits and we have obtained the explicit relation between our input functions and the Regge trajectories and vertex functions. Conversely, the values of the Regge parameters uniquely fix the model for all kinematic regions.

5. Applications

We have seen that our classical string model has a multiperipheral interpretation, with Regge asymptotic behaviour. In two-component duality [16], the mechanism of Figs. 2, 3 and 5 contributes only to the "resonant" or "cut-reggeon" cross-section,

$$\sigma_R \propto s^{\alpha_R(0)-1} \sim s^{-1/2}. \tag{5.1}$$

Accordingly we take $\alpha_{out} = \alpha_R(0)$. Thus, up to now the pomeron was not included. To obtain the "cut-pomeron" cross section,

$$\sigma_P \propto s^{\alpha_P(0)-1} \sim c^{st}, \tag{5.2}$$

we must take account of diagrams like the one of Fig. 7. This can be done in two possible ways: the first method is to use directly the classical string dynamics depicted in Fig. 8, which corresponds to the duality diagram of Fig. 7a. This yields a result in which the two darts of Fig. 7a decay independently, as in the dual parton model [17].

The second method goes beyond classical string dynamics. We generate the diagram of Fig. 7b by allowing the particles to be emitted either upward or downward in a random manner, with vertices which are obtained as before from Eq. (3.18) and (4.5)–(4.6), but with

$$\alpha_{\text{out}} = \alpha_P(0) = 1. \tag{5.3}$$

The second method has the advantage of generating not only cut-pomerons but also cut-reggeons as particular cases where particles are emitted all upward or all downward. This offers a refined way of doing "reggeon bootstrap" [18] by checking that

$$\frac{\text{number of cut-reggeon events}}{\text{number of cut-pomeron events}} \sim s^{\alpha_R(0)-\alpha_P(0)}. \tag{5.4}$$

The second method is also preferable theoretically: the first one, indeed, is equivalent to the double multiperipheral model represented in Fig. 9, with reggeized quark chain instead of ordinary reggeon chain. Thus the probability of a rapidity gap is governed by a Regge cut instead of a Regge pole. In short, the first method completely neglects the gluons exchanged between the two quark chains of Fig. 7b. It predicts no compensation of trans-

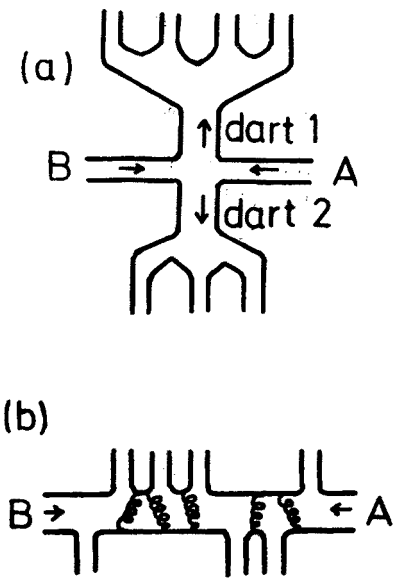

Fig. 7. Equivalent duality diagrams contributing to the "background" or "cut-pomeron" cross section (a) two-jet picture: the incoming strings A and B rearrange their quarks to form two "darts" D_1 and D_2 which subsequently decay. (b) multiperipheral picture. I have drawn some gluon lines as in Fig. 2b

verse momentum between a particle emitted by the upward chain and one emitted by the downward chain at the same rapidity (e.g., the K^+ and π^+ shown in Fig. 9), whereas the second method does predict a compensation.

Limitations to the accuracy of the model. Our classical model necessarily neglects the interferences between different multiperipheral diagrams. Since we are using planar dual diagrams (Figs. 2 and 7), these interferences are suppressed by powers of N_{flavour}^{-2}. If, instead, we had chosen multiperipheral diagrams where the exchanged reggeons have definite isospins and signatures (these diagrams are combinations of the former ones), the interference terms would have not been suppressed. Thus our choice minimizes the interference effects. On the other hand, our model generates factorized multi-Regge limits

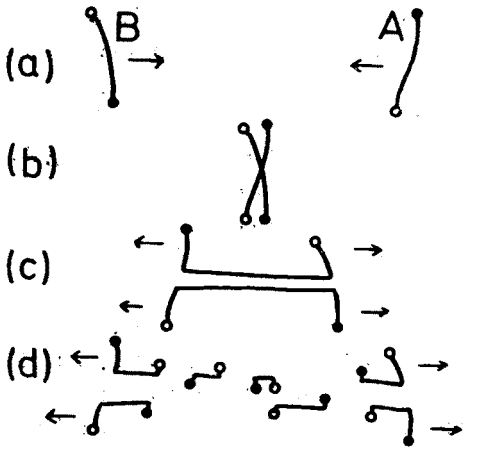

Fig. 8. Classical mechanism for the two-jet picture of Fig. 7a. As I did in Fig. 3, I have displayed the shapes of the strings at four different times. The difference comes from the "crossing over" shown in (b), which replaces the joining by the extremities

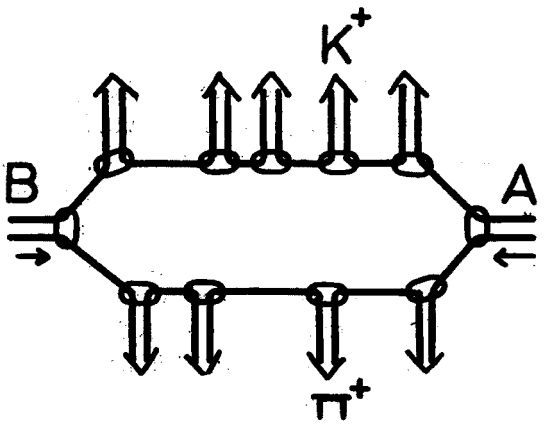

Fig. 9. Double multiperipheral model for the reactions contributing to the "cut-pomeron"; This model corresponds to the assumption that the two "darts" in Fig. 7a decay independently. It neglects the gluon exchanged between the two quark chains, displayed in Fig. 7b

for all diagrams, which is not true for the dual amplitudes without definite signatures [19]. This indicates a theoretical limitation of the model.

Finally, the factorization property illustrated by Fig. 6, and the inferred q^2 (or q'^2) independence of the splitting function, does not exactly account for the gluons exchanged vertically in Figs. 2b and Fig. 7b. These gluons have the effect of generating the hadron poles in the q_i^2 channels. This is particularly important in the case of pion exchange, due to the proximity of the pion pole; the actual pole contribution, in $(q'^2 - m_\pi^2)^{-2}$, is simulated in our model by $(\vec{q}'^2_T - m_\pi^2)^{-2}$, which is true only in the Regge limit.

6. Summary and conclusions

I have shown how classical string dynamics leads to a model for production of soft jets which contains the main qualitative properties of the multiperipheral model, including Regge asymptotic behaviour. Furthermore, there is a one-to-one correspondence between the functions which parametrize the model and those which parametrize Regge behaviour.

In high energy hadron-hadron collisions massive elongated strings are formed. At the classical level, their decays have the following three properties:

— limiting fragmentation, or Feynman scaling,

— factorization of the decay of a subsystem (Fig. 6),

— forward-backward symmetry.

The first two properties are based on causality + homogeneity of classical strings. They yield a fragmentation model of a recursive type, having a splitting function independent of q^2. The third property leads to the "symmetric Lund" solution.

Large longitudinal momentum transfers are suppressed by a factor $\exp(-b|q^+q^-|)$. This factor arises because a large value of $|q^+q^-|$ means that an unbroken string lives for a long time; this is an unlikely process.

Our recursive fragmentation model yields multiparticle states corresponding either to cut reggeons or to the sum of cut pomerons + cut reggeons. In the second case, one avoids the decomposition of a pomeron jet into two independent quark jets, which has no theoretical justification.

The model is at variance with the idea of "topological jet universality" [20] which relates, for instance, a cut-reggeon jet to a $q\bar{q}$ jet in e^+e^- annihilation. The latter process is not determined by Regge theory. On the other hand, triple-Regge behaviour yields a leading particle spectrum in a cut-reggeon jet which behaves like $(1-z)^{-1/2}$ at $z \to 1$; this contrasts with the $(1-z)$ or $(1-z)^2$ behaviour observed in quark jets.

The main limitations of the model are the following: a) Spin degrees of freedom have not been included. b) Interference terms are neglected. We have minimized the interference effects by taking planar multiperipheral diagrams instead of diagrams where the exchanged reggeons have well-defined isospin and signatures. This procedure has errors which are only of order $1/N^2_{\text{flavour}}$. c) The pion pole appears in the variable $\vec{q}_T^2$ because we neglected the q^2 dependence of the splitting function.

In spite of the above limitations, the classical string model described here has the advantage over other often used models in that it accounts for longitudinal softness ($|q^+q^-|$

damping), forward-backward symmetry and Regge asymptotic behaviour. It can be applied to any physical situation where soft jets occur such as the following : deep inelastic reactions having "spectator jets"; reactions producing high mass diffractive states (triple-Pomeron mechanism); reactions with several "cut-pomerons" which are becoming important at present accelerator energies. These particular processes are not naturally described by the two-component duality model.

I wish to thank Zakopane Summer School for having given to me the opportunity to give this review lecture, and I am indebted to Martial Baker for his valuable help in the final form of the manuscript.

REFERENCES

[1] D. Amati, S. Fubini, A. Stanghellini, M. Tonin, *Nuovo Cimento* **22**, 569 (1961); D. Amati, A. Stanghellini, S. Fubini, *Nuovo Cimento* **26**, 896 (1962).
[2] A. Krzywicki, B. Petersson, *Phys. Rev.* **D6**, 924 (1972); J. Finkelstein, R. D. Peccei, *Phys. Rev.* **D6**, 2606 (1972).
[3] R. D. Field, R. P. Feynman, *Nucl. Phys.* **B136**, 1 (1978).
[4] B. Andersson, G. Gustafson, B. Söderberg, *Z. Phys. C — Particles and Fields* **1**, 105 (1979).
[5] See, for instance, J. Scherk, *Rev. Mod. Phys.* **47**, 123 (1975).
[6] X. Artru, G. Mennessier, *Nucl. Phys.* **B70**, 93 (1974).
[7] X. Artru, *Phys. Reports* **97**, 147 (1983).
[8] X. Artru, LPTHE Orsay 79/8, (1979).
[9] See, for instance, B. Andersson, G. Gustafson, G. Ingelman, T. Sjöstrand, *Phys. Reports* **97**, 31 (1983), pages 68–72 and references therein.
[10] J. D. Bjorken, in Proc. SLAC Summer Institute on Particle Physics, SLAC-167 (1973) vol. I, p. 1.
[11] M. G. Bowler, *Z. Phys. C — Particles and Fields* **11**, 169 (1981).
[12] M. G. Bowler, *Z. Phys. C — Particles and Fields* **22**, 155 (1984).
[13] X. Artru, *Z. Phys. C — Particles and Fields* **26**, 83 (1984).
[14] C. Quigg, P. Pirilä, G. H. Thomas, *Phys. Rev. Lett.* **34**, 290 (1975); A. Krzywicki, C. Quigg, G. H. Thomas, *Phys. Lett.* **57B**, 369 (1975).
[15] X. Artru, LPTHE Orsay 85/23 (1985).
[16] P. G. O. Freund, *Phys. Rev. Lett.* **20**, 235 (1968); H. Harari, *Phys. Rev. Lett.* **20**, 1395 (1968).
[17] A. Capella, U. P. Sukhatme, Chung-I Tan, J. Tran Thanh Van, *Phys. Lett.* **81B**, 68 (1979); H. Minakata, *Phys. Rev.* **D20**, 1656 (1979); G. Cohen-Tannoudji, A. El Hassouni, J. Kalinowski, O. Napoly, R. Peschanski, *Phys. Rev.* **D21**, 2699 (1980); A. B. Kaidalov, K. A. Ter-Martirosyan, *Yad. Fiz.* **39**, 1545 (1984) [*Sov. J. Nucl. Phys.* **39**, 979 (1984)]. See also Ref. [6].
[18] H. Lee, *Phys. Lett.* **30**, 719 (1973); Chang-Hong-Mo, J. E. Paton, *Phys. Lett.* **46B**, 228 (1983).
[19] J. H. Weiss, *Phys. Rev.* **D4**, 1777 (1971).
[20] For a discussion of topological jet universality, see X. Artru, *Phys. Rev.* **D29**, 840 (1984).